Research Article

Nevil Wickramathilaka*, Uznir Ujang, Suhaibah Azri, and Tan Liat Choon

Three-dimensional visualisation of traffic noise based on the Henk de-Klujijver model

https://doi.org/10.1515/noise-2022-0170
received February 10, 2023; accepted August 10, 2023

Abstract: Visualisation of road traffic noise is vital for traffic noise planning policies. Several factors affect the noise from road traffic with physical and environmental conditions. Collecting noise levels around the world is not a possible task. Therefore, calculating noise levels by a valid noise model, and spatial interpolations, is prime to traffic noise visualisation. In this study, the Henk de Klujijver noise model is used. Designing noise observation points (Nops) embedding with a three-dimensional (3D) building model and identifying the best suitable spatial interpolation are important to visualise the traffic noise accurately. However, interpolating noise in 3D space (vertical direction) is a more complex process than interpolating in two-dimensional (2D) space. Flat triangles should be eliminated in the vertical direction. Therefore, the structure of Nop has a major influence on spatial interpolation. Triangular Irregular Network (TIN) interpolation is more accurate for visualising traffic noise as 3D noise contours than Inverse Distance Weighted and kriging. Although kriging is vital to visualise noise as raster formats in 2D space. The 3D kriging in Empirical Bayesian shows a 3D voxel visualisation with higher accuracy than 3D TIN noise contours.

Keywords: traffic noise model, designing noise observation points, spatial interpolation, noise visualisation, accuracy validation

*** Corresponding author: Nevil Wickramathilaka**, 3D GIS Research Lab, Faculty of Built Environment and Surveying, Universiti Teknologi Malaysia, 81310, Johor Bahru, Johor, Malaysia; Southern Campus, General Sir John Kotelawala Defence University, Edison Hill, Nugegalayaya, Sewanagala, Sri Lanka, e-mail: nevilvidyamanee@kdu.ac.lk
Uznir Ujang, Suhaibah Azri, Tan Liat Choon: 3D GIS Research Lab, Faculty of Built Environment and Surveying, Universiti Teknologi Malaysia, 81310, Johor Bahru, Johor, Malaysia

1 Introduction

Compared to other environmental and urban noise, such as industry, airplanes, railroads, or recreational activities, the problem of exposure to road traffic noise has been worse recently [1–3]. Identifying factors for road traffic noise [4–6], selecting a suitable road traffic noise equation to calculate road traffic noise levels [7], spatial interpolation of road traffic noise levels [8,9], validation of interpolated road traffic noise levels [9,10], and colour notifications for visualisation [11] are the main issues in road traffic noise visualisation in three dimensional (3D) space [12]. Different factors affect road traffic noise levels [13]. Recently, different types of road traffic models have been associated with calculate road traffic noise levels [14]. Road traffic noise zones are vital for identifying noise-risky areas [13]. Urban road traffic produces noise primarily through the interaction of tires and the road surface [15,16]. Additionally, speed and traffic flow conditions impact road traffic noise [14,17,18]. Moreover, the noise of tyres, construction of road, road surface conditions [18], noise generation mechanism, measurement methods, and accuracy of the validation affect road traffic noise levels [19].

Furthermore, distance between noise vehicles to observation points, ground coverage, and reflectance from building facades are various factors for road traffic noise pollution [20]. Furthermore, the acoustic performance of a pavement [21] plays an important role. Recently, most studies have focused on identifying pavement performance for road traffic noise pollution [3]. For these studies, the Statistical Pass-By (SPB-ISO) method and Close Proximity Index (CPX) method have been embedded [17]. However, the current study focusses on identifying road traffic noise levels in two-dimensional (2D) and 3D space. Therefore, additional road traffic noise conditions should be considered rather than SPB-ISO.

Various types of road traffic noise calculation methods have been used to calculate noise levels in 3D. The United Federal Highway Administration traffic noise model (FHWA), the road traffic noise model (CoRTN) in the United Kingdom, the RLS-90 model of Germany, and the Henk de Klujijver

model [20,22] are prominent for 3D road traffic noise visualisation. The CNOSSOS-EU model of the European Union can be one of the latest road traffic noise models. Recently, several studies have used the calculation of CNOSSOS-EU model for the road traffic noise. Tyre and road interaction, diffraction during propagation, traffic flow, average speed, and ground effects are the parameters of this model. However, noise reflection from the buildings and the barriers, impact of barriers, and weather conditions are not considered in the CNOSSOS-EU model [23]. This model implies a closer connection to reality. However, the propagation of road traffic noise along the vertical direction is not considered here. There is a lack of 3D road traffic noise mapping through the CNOSSOS-EU model. To avoid these issues, the Henk de Klujijver road traffic noise model is used in this current study. Traffic flow, different categories of vehicles, ground absorption, noise absorption by air, noise reflection from the barriers, weather conditions, and impact of noise barriers are considered in the Henk de Klujijver road traffic noise model. Furthermore, several studies have used this model for the 3D road traffic noise mapping in urban cities [20].

Collecting noise levels everywhere is not a possible process [24]. Calculating the noise levels where the designed noise observation points (Nops) on the 2D and 3D space *via* the noise equation is an effective method. Applying spatial interpolation on noise levels is possible to create a continuous noise surface [8]. There are two main components in traffic noise interpolation: designing Nops in 3D space and applying a proper spatial interpolation technique [8]. The energy of the noise levels decreases from the noise source to the receiver while propagating [21]. This means that the distance between the noise source and the receiver affects inversely on road traffic noise levels [23,25]. Determining the interval between Nops, what is the maximum distance that needs to be maintained between the receiver and the noise source, and designing Nops along uphill and downhill areas (90° slope) are still issues in road traffic noise mapping [26]. However, identifying the impact of the interval of Nops along the horizontal and vertical directions (3D space) is prime for noise interpolations [27].

Embedding well-structured Nops with a noise equation enhances the accuracy of noise interpolation. Inverse Distance Weighted (IDW), kriging, and Triangular Irregular Network (TIN) are the spatial interpolation techniques that are used in traffic noise mapping widely [8,28]. The attributes of a Nop (x-coordinate, y-coordinate, z-coordinate, and noise level) are exposed to the interpolation, algorithm, and it seems to be a four-dimensional (4D) spatial interpolation [29,30]. Therefore, the interpolation of road traffic noise in a 3D space is a complex process because every height value (z) consists of a noise value [31]. Noise contours and raster noise surfaces are prime for visualising road traffic noise in 3D space [32–34]. TIN is generally used to interpolate traffic noise levels along the vertical direction, and IDW and kriging are vital for interpolating on the horizontal surface. The design structure of noise points along the vertical direction is important for removing flat triangles (different (z) values for the same (x) and (y) coordinates) for the interpolated surface [35]. Especially, 3D kriging using empirical Bayesian kriging allows us to interpolate four parameters in 3D space [30]. It creates 3D multidimensional geostatistical layers along the vertical direction. Therefore, 3D kriging can be adopted to identify vertical propagation of road traffic noise levels *via* 3D visualisation. Moreover, 3D kriging can be embedded with 3D voxels [36–38]. In this current study, it shows the development of IDW, kriging, and TIN spatial interpolations to interpolate road traffic noise levels in 3D space *via* 3D road traffic noise contours. Furthermore, 3D kriging is embedded with 3D voxels to visualise road traffic noise *via* raster format. Furthermore, the existing Henk de Klujijver road traffic model is formulated with other significant equations to consider road traffic noise factors. In addition, this study aims to demonstrate such 3D road traffic noise visualisation errors, accuracy comparison of different interpolation techniques, and accuracy comparisons of different types of 3D visualisation.

To address the aforementioned issues, Univeristi Teknologi Malaysia (UTM) was selected as the study area, and UTM is located in Johor City, Malaysia. Noise pollution from road traffic is increasing in UTM premises day by day due to developments [39]. Recently, there is latest commercial software for 3D road traffic noise mapping. However, ArcGIS Pro software provides several significant tools for 3D interpolation and 3D visualisation. Even for 3D interpolation and 3D voxelisation, ArcGIS Pro provides significant facilities. Furthermore, ArcGIS Pro provides capabilities to integrate a 3D building model and a 3D road traffic noise visualisation. Therefore, the current study uses ArcGIS Pro for the 3D visualisation of road traffic noise. Mainly, Geographic Information System (GIS) approaches are shown for road traffic noise visualisation.

2 Methodology

2.1 Study area

The location of the study area is 1°33′37.6″N 103°38′16.4″E, and it is located at UTM, Johor, Malaysia. This study is carried out to determine the noise levels of the UTM. According to previous studies, average noise levels have been identified to be about 70 dB(A) around the faculty building areas in the morning and evening. When considering

Figure 1: Research study area (source: Google Earth).

the inner circle area of the university, the average traffic noise levels range from 65 to 70 dB(A) [39]. Figure 1 illustrates the overview of the study area.

The flow chart of the study is shown in Figure 2, and the study is conducted in phase 1, phase 2a, phase 2b, and phase 3 to meet the objectives and requirements.

2.2 Data preparation

2.2.1 Number of vehicles, vehicle speed, and noise levels

The number of vehicles, the speed of vehicles, and the type of vehicles (light, medium, and heavy vehicles) were considered. According to the capacity of the engine, the vehicles were classified as light, medium, and heavy. Engine capacity less than 2,000 cc (cc is the unit to measure engine capacity) was considered for light vehicles. The cars were taken as light vehicles. Engine capacity between 2,000 and 3,000 cc was considered for medium vehicles. Vans, jeeps, and cabs were considered medium vehicles. If the engine capacity is greater than 3,000 cc, vehicles such as a lorry, bus, and canter were considered heavy vehicles. Vehicles have been counted manually for about 10 (20) days from 7.30 a.m. to 9.30 a.m. (during peak traffic times in UTM). The road network is divided into 13 road segments to easily count vehicles. Road segments are shown in Figure 3, and the number of vehicles in the corresponding road segments is illustrated in Table 1. The speed of vehicles is vital to calculate road traffic noise levels, and it is very difficult to find the speed for each vehicle separately [40]. Therefore, the average speed of the vehicle was considered, after examining ten vehicles in each class. To observe noise levels, the DEKKO SL-130, sound level meter, was used. The accuracy of this noise meter is ±0.3 dB(A) (decibel). A handheld global position system (GPS) instrument (±1–3 m) was used to observe the noise points of the location of the validation sample noise points.

2.3 Formulate an equation for traffic noise calculation

The Henk de Klujijver noise model was adopted to visualise traffic noise. According to previous studies, this equation

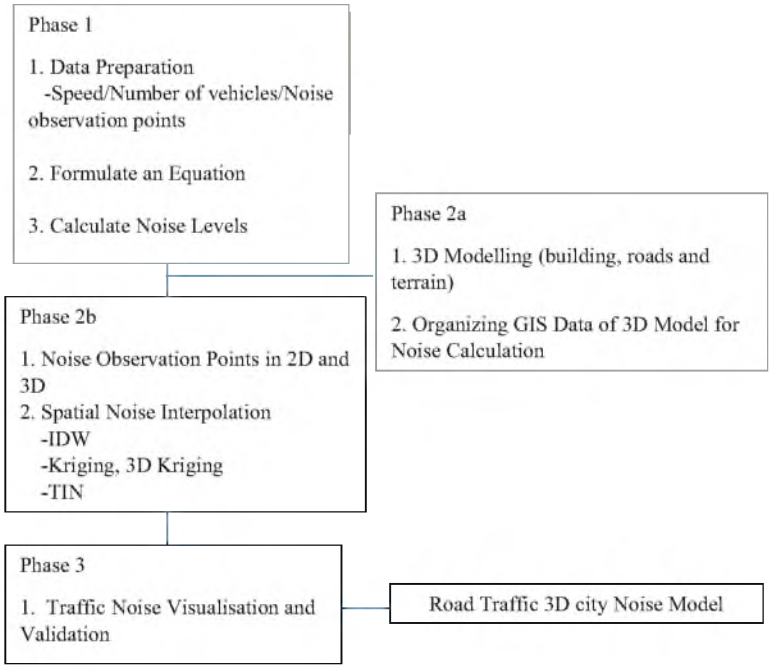

Figure 2: Research workflow.

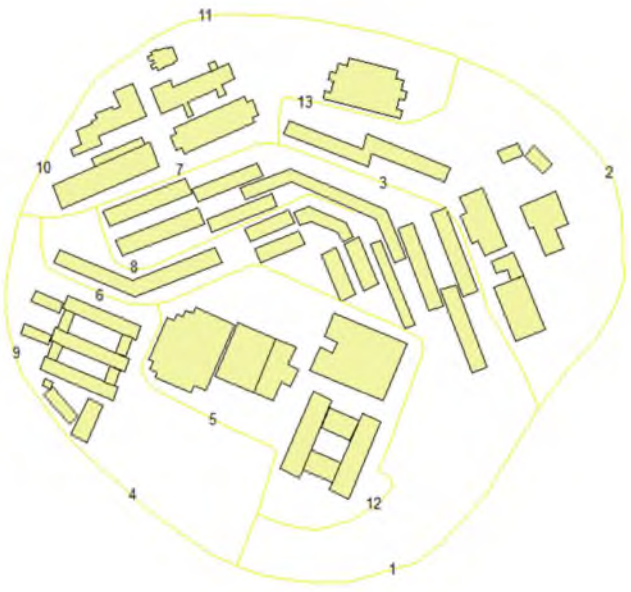

Figure 3: Numbered road segments according to the flow of traffic in the morning.

has been used in the Hemmat highway in Iran to traffic noise embedded with the 3D building model. This model considers different factors for road traffic noise, such as the number of vehicles, speed of vehicles, noise reflectance of building facades, noise absorption by air and ground, wind effect, and noise absorption by road surface. However, it does not consider changes in noise levels with temperature [41] and pressure [42], and noise absorption by building facades [43]. Therefore, the study was carried out without the aforementioned parameters. Furthermore, this equation assumes that noise comes from the road's centreline, and the receiver point will be exposed to the highest noise levels when it makes the shortest distance between the receiver point and the noise source. Eq. (1) describes the Henk de Klujijver noise model [20].

$$L_{\text{Aeq}} = E + C_{\text{optrek}} + C_{\text{reflectie}} - D_{\text{afstand}} - D_{\text{lucht}} - D_{\text{bodem}} - D_{\text{meteo}} - D_{\text{barrier}}. \quad (1)$$

L_{Aeq} is the noise level of the calculation point, and E is the noise emission level. E can be calculated as the following Eq. (2), E_{lv} is the noise of light vehicles, E_{mv} is the noise of medium vehicles, and E_{zv} is the noise of heavy vehicles, which can be seen in Eqs. (3)–(5). V_{lv}, V_{mv}, and V_{zv} are the average speeds of light, medium, and heavy vehicles. Q_{lv}, Q_{mv}, and Q_{zv} light, medium, and heavy vehicles.

$$E = 10 \times \log\{(10^{E_{\text{lv}}}/10) + (10^{E_{\text{mv}}}/10) + (10^{E_{\text{zv}}}/10)\}, \quad (2)$$

$$E_{\text{lv}} = 69.4 + 27.6 \times \log\{V_{\text{lv}}/V_{\text{o}}\} + 10\log\{Q_{\text{lv}}/V_{\text{lv}}\} + C_{\text{wegdek,lv}}, \quad (3)$$

$$E_{\text{mv}} = 73.2 + 19.0 \times \log\{V_{\text{mv}}/V_{\text{o}}\} + 10\log\{Q_{\text{mv}}/V_{\text{mv}}\} + C_{\text{wegdek.mv}}, \quad (4)$$

$$E_{\text{zv}} = 76.0 + 17.9 \times \log\{V_{\text{zv}}/V_{\text{o}}\} + 10\log\{Q_{\text{zv}}/V_{\text{zv}}\} + C_{\text{wegdek.zv}}, \quad (5)$$

where C_{wegdek} is the noise emission from the road surface due to friction between the tire and the road surface. Δlm and bm are the constant values for different road's surfaces. Eq. (6) shows the following:

$$C_{\text{wegdek}} = \Delta\text{lm} + \text{bmlog(vm/vom)}, \quad (6)$$

where C_{oprek} is the extra noise emission from vehicle braking and accelerating. $C_{\text{reflectie}}$ is the noise reflexion of building facades and wall barriers. Fobj is the reflection noise on the other side of the road and is between 0 and 1. Only the object is situated at a reasonable distance, and it will be considered reflective noise. Eq. (7) describes the reflectance noise from the other side of the road.

$$C_{\text{reflectie}} = 1.5 \times \text{fobj}. \quad (7)$$

The traffic reflexion of traffic noise from building facades and other hard surfaces affects the mitigation of the noise levels [44]. The noise reflection from opposite side facades and rigid surfaces of the opposite side is $+1.5 \times (\theta'/\theta)$ dB(A), where θ' is the sum of angles subtended from facades and surfaces. θ is the total angle subtended from road the segments to the receiver point [20,45]. This basic theory can be embedded to find the value of fobj (7). Figure 4 illustrates the traffic noise reflection correction with building facades.

According to the UTM building structure, many buildings are located on both sides of the road. Therefore, it

Table 1: Number of light, medium, and heavy vehicles on the corresponding road segments in the morning

Road segment	1	2	3	4	5	6	7	8	9	10	11	12	13	14
L	125	127	166	671	277	321	241	56	433	230	459	99	51	17
M	10	11	7	24	11	17	17	9	21	8	8	9	3	2
H	34	21	19	18	0	0	31	0	53	15	14	0	0	0

L: light vehicles, M: medium vehicles, H: heavy vehicle.

seems that the sum of angles subtended from opposite side facades to a receiver point is laid as the continuous angle. Thus, it can be concluded that the ratio between the sum of the subtended angle and the total subtended angle is one. According to this verification, the noise reflection correction was determined as +1.5 dB(A). D_{afstand} is the reduction of noise with distance. D_{lucht} is the reduction of the noise due to absorption from the air. r is the displacement between the noise source and the observation point. Eqs. (8) and (9) show how to calculate reduction noise and absorption noise.

$$D_{\text{lucht}} = 0.01 \times r^{0.9}, \tag{8}$$

$$D_{\text{afstand}} = 10\log(r). \tag{9}$$

D_{bodem} is the traffic noise absorption from the ground, where B is the part between the centreline of the road and the Nops. The value of B is between 0 and 1. The h_{w} is the height of the traffic Nop from the reference ground level. The h_{weg} defines the height of the road from ground level. Eq. (10) shows that

$$D_{\text{bodem}} = B[2 + 4(1 - e^{-0.04r}) \times (e^{-0.65h_{\text{w}}} + e^{-0.65(h_{\text{weg}}-0.75)})]. \tag{10}$$

The impact of ground attenuation is a result of noise absorption [20]. Ground attenuation on traffic noise levels does not affect the size of the region (size of the part between the noise source and the receiver) and depends on the properties of the ground surface. For hard ground (dense asphalt, concrete), the B is 0. The B is 1, when the ground is completely covered by grass (porous ground) [46]. B is between 0 and 1 when the ground is covered with both porous and hard ground. B is 0.7 for compacted lawns, and it is 0.3 for the gravel areas [47]. Therefore, the aforementioned value of B was attached to the research with the field verification of ground surfaces in the UTM area. D_{meteo} represents the reduction in noise due to wind conditions, and it is shown in Eq. (11) [20].

$$D_{\text{meteo}} = 3.5 - 3.5e^{(-0.04r/(h_{\text{weg}}+h_{\text{w}}+0.75))}. \tag{11}$$

2.4 3D City model

The traffic network is essential for the sustainable development of urban cities [48]. Traditionally, road traffic noise was visualised in a 2D space with embedding geographical information science (GIS) [49]. Recently, 3D GIS has emerged for road traffic noise visualisation [50,51]. The simple building model and the complex building model are the two types of models inserted with traffic noise visualisation. Due to the travel of noise in every direction, a 3D building model is vital [52]. However, a simple building model of a city is enough for visualisation of traffic noise [53]. A simple building model of the UTM area was captured from a drone survey. Buildings, road centreline, and digital elevation models are extracted after the classification of drone point clouds [54]. Figures 5 and 6 show point clouds and the 3D model of UTM. Pix4d Mapper, ArcGIS Pro, and Civil 3D software were used for 3D modelling.

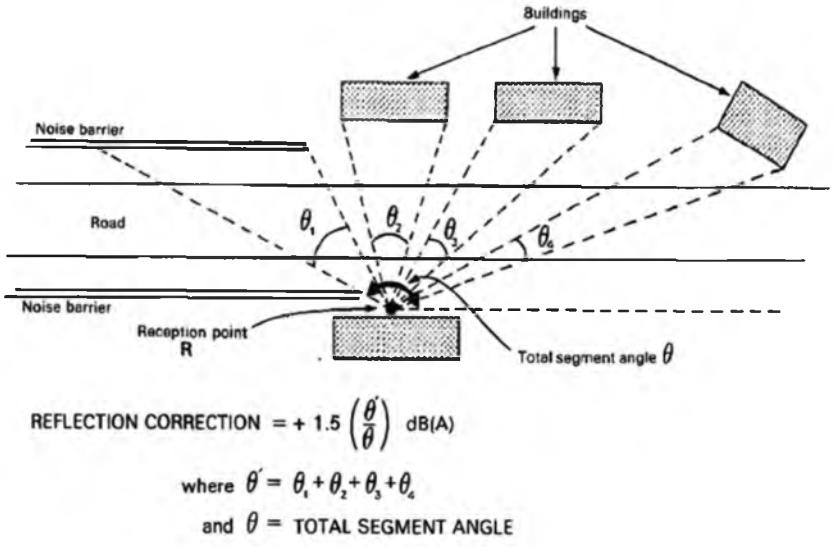

Figure 4: Noise reflection correction which happens from buildings and barriers on opposite sides of roads [45].

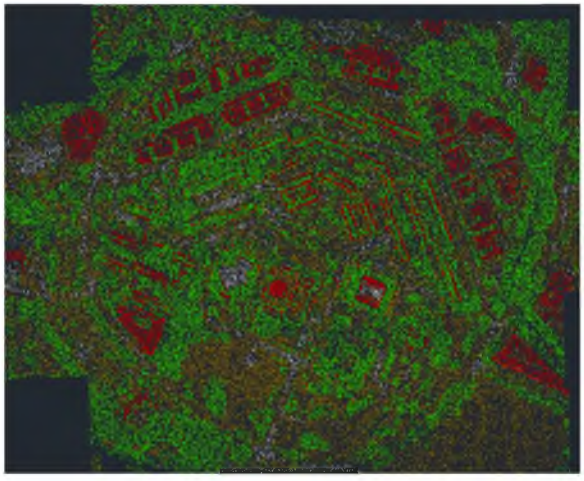

Figure 5: Drone point clouds to design 3D buildings of study area.

2.5 Design of traffic Nops and spatial interpolation

2.5.1 Nops design

Nops are designed in 2D and 3D space as grid patterns [55]. It is vital for continuous surface during spatial interpolation [56]. The Nops were designed along the shortest distance between the vehicle and the centreline of the road [9]. According to the Henk de Klujijver noise model, the noise mitigated from 10log(r); r is the shortest distance between the vehicle and Nop. Therefore, the distance interval between Nop was 2 m. If the study area is approximately flat, it is not a complex process to establish Nop compared to the undulated areas. Noise travels in all directions, including upward and downward. If the slope of the terrain is straight down and straight up (90°), it is a reason to mitigate noise levels from the terrain barriers [57]. The area of UTM is large and undulated, and there are up and down slopes. Therefore, the Nops were not designed beyond the up and straight down slopes, as shown in Figure 7. Still, there is no method to identify the maximum distance that the noise can travel. In the pilot survey, the mean noise levels were 63.6 dB(A) to the nearest road edge, and the average traffic noise levels were 41.4 dB(A) without any vehicles. It is about 22 dB(A) noise reduction. Therefore, under the verification of 10log(r), the distance of 100 m was not exceeded to design Nop. There was no special reason to select the distance interval of Nop along the parallel direction with the road [9]. To maintain accuracy, 10 m was manipulated for Nop. Nop in 2D space is illustrated in Figure 7. Flat triangles (same x and y coordinates for different z coordinates) were eliminated when designing Nop along the vertical axis [9]. If the Nops have the same x and y coordinates for different z values along the same vertical direction, this is an issue for spatial interpolation. The first Nop was designed 1 m away from the building façade, then the other Nop was designed 10 cm away from the previous position. The points' intervals of the 3D space (along the vertical axis) were the same as those of the 2D space. Figure 7 illustrates Nop in 3D space.

2.5.2 Spatial interpolation and traffic noise visualisation

TIN, IDW, and kriging spatial interpolation techniques were used to interpolate noise levels. Furthermore, the 3D kriging spatial interpolation technique was adopted in this study for interpolation. The distance-weighted factor

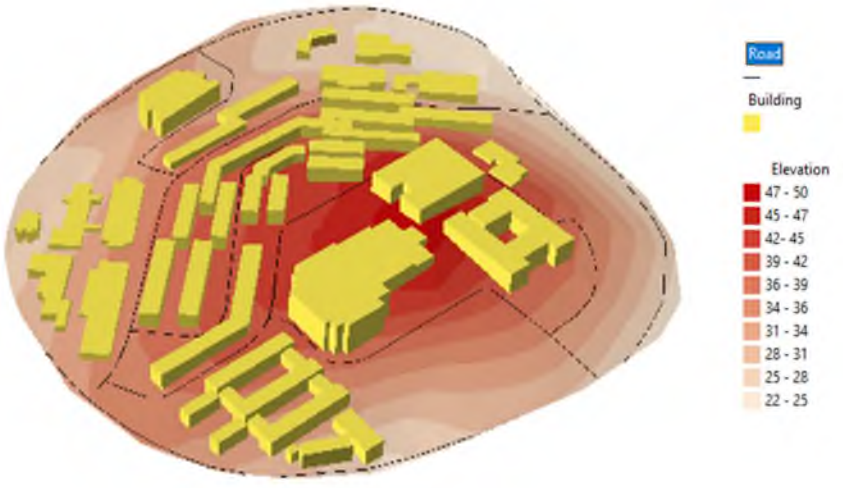

Figure 6: 3D building model of study area including terrain variation.

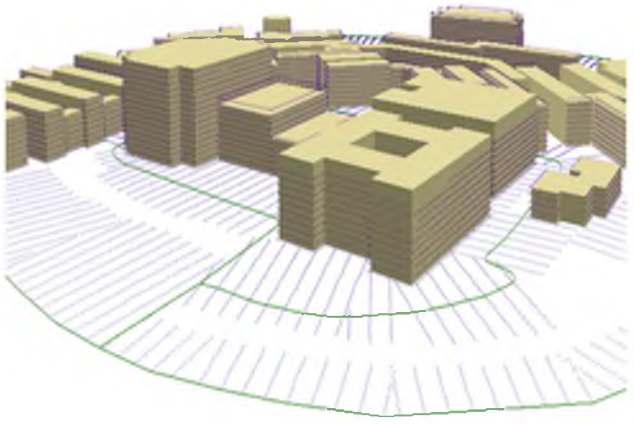

Figure 7: Designed Nops along facades of buildings and horizontal direction in 3D space.

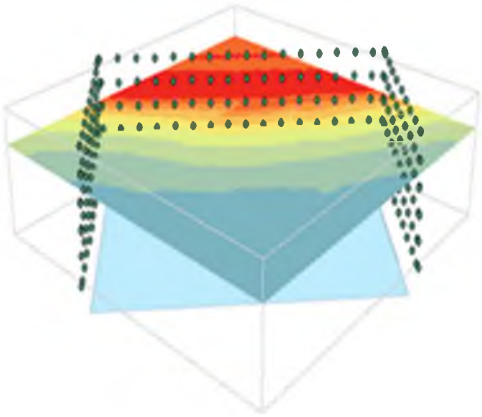

Figure 8: 3D Kriging horizontal slices for road traffic noise levels in 3D space.

was taken as two for IDW interpolation. It means that a second-order polynomial function was attached to IDW. Variogram and the Gaussian method were applied for kriging [8,9]. Cell size was taken as 1 m to visualise the noise level in raster format on 2D space. The TIN interpolation technique was more applicable for noise interpolation in the vertical direction (3D space) than IDW and kriging [9]. However, it was not easy to interpolate on the vertical axis. A Nop in 3D space has four parameters, such as the x coordinate, the y coordinate, z coordinate (heights along the building, facades), and the dB(A) value [57]. TIN, IDW, and kriging are applicable to work with three parameters in spatial interpolation. Because Nops were designed on the vertical axis to eliminate flat triangles (the same x and y coordinates for different z coordinates on the same vertical axis), it was the reason to project Nops to 2D space without overlapping. Using x and y coordinates with dB(A) values, Nop was interpolated in 2D space using TIN. Thus, the TIN surface was converted into noise contours (contour interval 0.2 dB(A)), and then, z values (heights along building the façade) were inserted using ArcGIS Pro software. To improve the visual quality of the noise visualisation, the 3D voxel-based method was adopted to represent the traffic noise levels in the 3D space. The 3D kriging used in Empirical Bayesian Kriging allows one to assign four parameters (including dB(A), values), and it shows the noise levels as horizontal slices along the vertical axis (Figure 8). The collection of these 3D kriging layers is vital for voxel cube representation [58].

2.6 Validation of interpolated traffic noise levels

Validation of interpolated road traffic noise levels with sample Nops is vital in both 2D and 3D space using a statistical method. Root mean square error (RMSE) and mean error (ME) were used to validate road traffic noise in 2D and 3D [9]. The sample points were observed in 2D and 3D. The number of sample points, the distribution, and the density of the sample points were considered. To observe 2D road traffic sample noise levels, the noise level metres were kept 1.5 m high from the ground level. To observe the noise levels of the 3D road traffic sample, the noise level metres were kept along the facades of the buildings, and the distance interval between the noise level metres is 4.5 m along the vertical direction. The lower RMSE and ME were kriging surfaces rather than IDW and TIN surfaces. Therefore, interpolated noise surfaces from kriging were used to visualise traffic noise levels in 2D. Visualisation of kriging noise is illustrated in Figure 9. Colour notifications are vital for noise visualisation: purple was used to represent higher noise levels, and light blue was used to represent lower noise levels [11]. According to the rules and regulations of the World Health Organisation, 55 dB(A) is not exceeded [59]. Therefore, the 2D noise visualisation was reclassified as <55 dB(A) and >55 dB(A). The reclassified 2D noise visualisation is shown in Figure 10. Moreover, the 3D kriging voxel, visualisation, and the 3D noise contour visualisation are shown in Figures 11 and 12. The reclassified noise contours are shown in Figure 13.

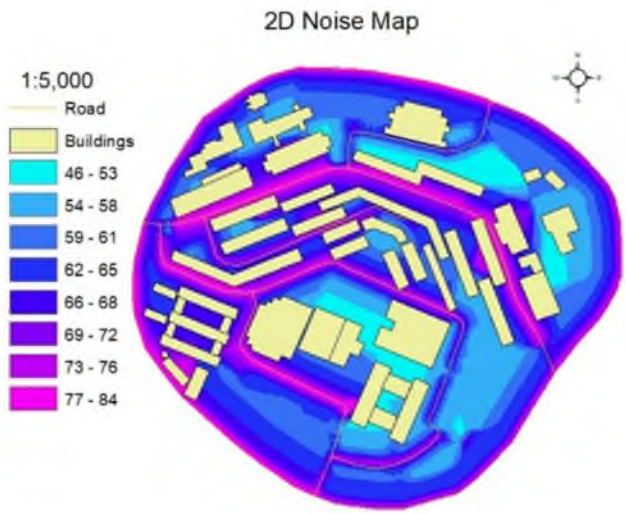

Figure 9: 2D road traffic noise map.

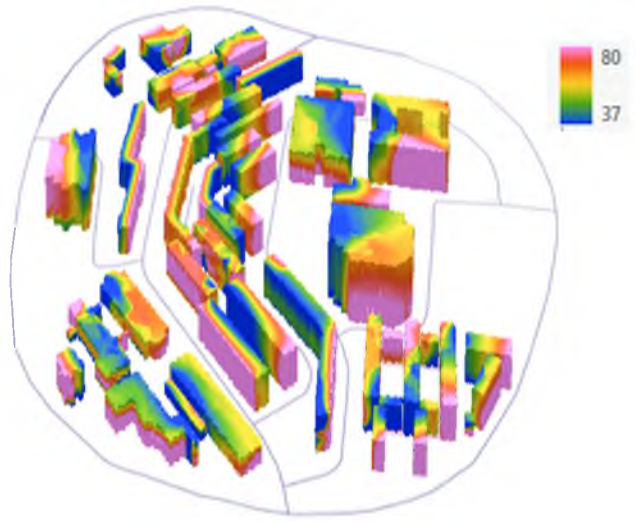

Figure 11: 3D voxel road traffic noise visualisation by combining 3D kriging noise layers.

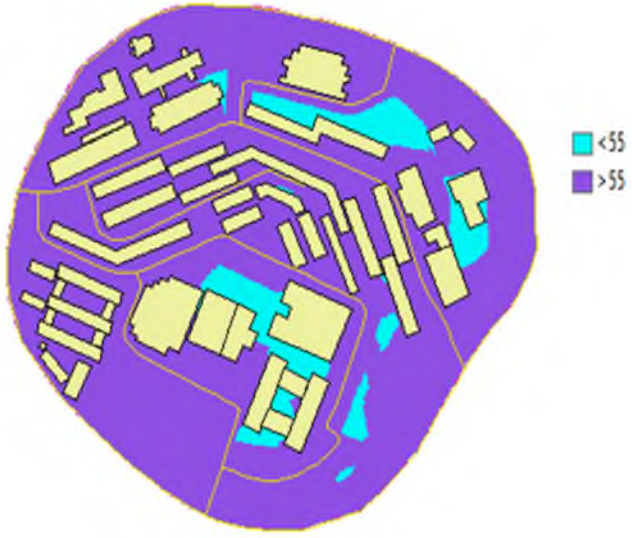

Figure 10: 2D reclassified road traffic noise map with concerning lower than and greater than 55 dB(A).

3 Results and discussion

Traffic noise levels are higher on roads than in other areas. However, the number of heavy vehicles has a significant influence on increasing traffic noise levels. According to Figure 9, when considering road segments 6 and 7, there is a considerable difference in the number of heavy vehicles. It seems that the noise levels around segment 7 of the road are higher than those around segment 6. According to Figure 10, the noise levels are greater than 55 dB(A) in many buildings. However, few buildings are within an area of less than 55 dB(A). The area (less than 55 dB(A)) is 36,512 m^2, and the area (more than 55 dB(A)) is 331,873 m^2. Traffic noise decreases with distance, but the rate increases as the ground consists of grass. Noise validation in 2D kriging is as follows: ME is −0.301 and RMSE is 1.628. IDW shows that ME is −0.405 and RMSE is 2.316. TIN results show that ME is −0.418 and RMSE is 2.915. Ninety-seven sample noise points were used to validate 2D noise visualisation. The kriging is a geostatistical spatial interpolation technique. The correlation among Nops is considered. Therefore, kriging is vital to interpolate clusters and large sizes of data. Moreover, according to the variance of the Nops (decreasing the similarity between Nops with the distance), the mathematical model is fitted to semi-variance points. This model can be called a variogram. The Gaussian variogram was used in kriging. The IDW is a deterministic method. The main influencing factor for IDW is its weighting factor. If the weighting factor is increased, the interpolated surface is smoothed. The weighting factor describes the significance between an interpolated value and an observed value. However, when this weighting factor is used, the interpolated value is the same as the observed value. Then, it is a reason for a less accurate interpolated surface. Therefore, the weighting factor of the IDW was selected as 2. When considering traffic noise levels, there is no higher value difference between Nops, and it is about 1 dB(A) for 1 m. Thus, there is a correlation between the Nop values. Therefore, kriging shows better accuracy than IDW and kriging in the 2D traffic noise mapping.

The distance interval of the Nop depends on the traffic noise model. Traffic noise reduces from 10log(r) with the distance in the Henk de Klujijver noise model. If the distance interval is 1 m between two Nops, according to that equation there is no noise reduction. Therefore, the

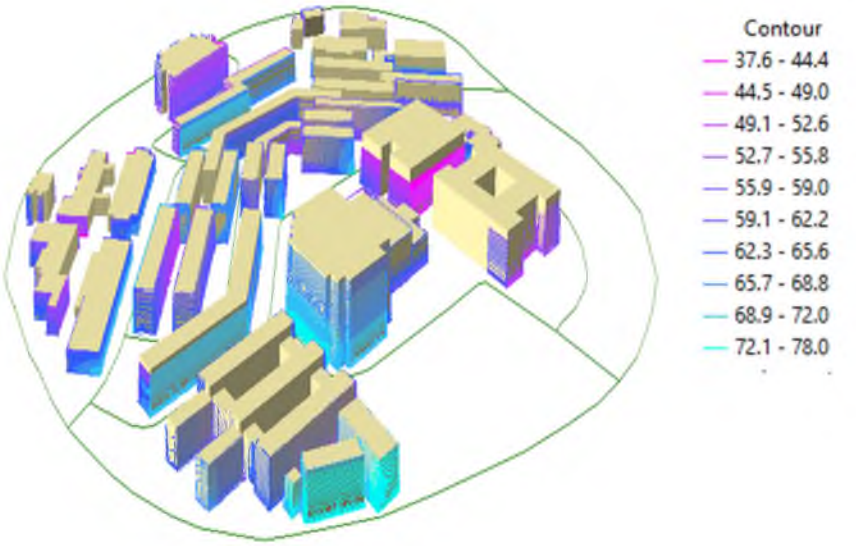

Figure 12: 3D road traffic noise contours visualisation along the facades of buildings.

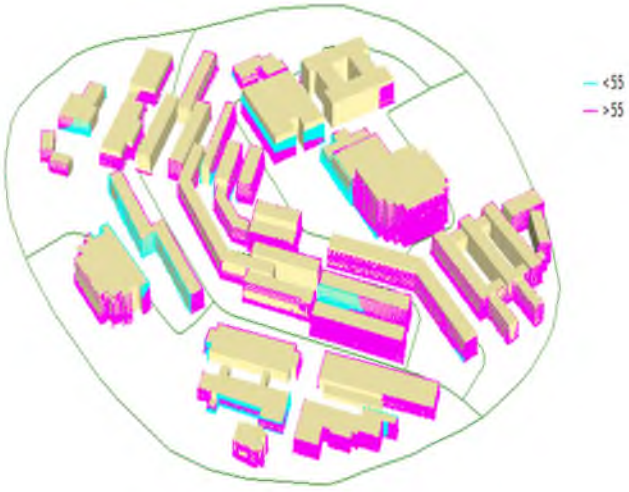

Figure 13: 3D reclassified road traffic noise contours with concerning lower than and greater than 55 dB(A).

distance interval between Nop is vital, 2 m. Designing Nop as eliminating flat triangles (the same x and y coordinates for different z coordinates) is important to interpolate noise levels in the vertical axis. However, according to the results in the 3D interpolation, there is no more difference between the values of Nops along the vertical axis; it is about 0.2 dB. However, the IDW and kriging noise contours are inaccurate on the vertical axis, and there are some irregular and unpredictable structures (such as the sin wave). It means that IDW and kriging noise contours do not exactly fit with the Nop on building facades (Figure 14(a)–(c)). The TIN contours were directly extracted from a TIN interpolation. The kriging and IDW noise contours were designed after converting the TIN surface to the IDW and raster surfaces. But the TIN contours are exactly fit with Nops. Therefore, adopting TIN spatial interpolation techniques is vital for noise interpolation in the vertical axis rather than IDW and kriging.

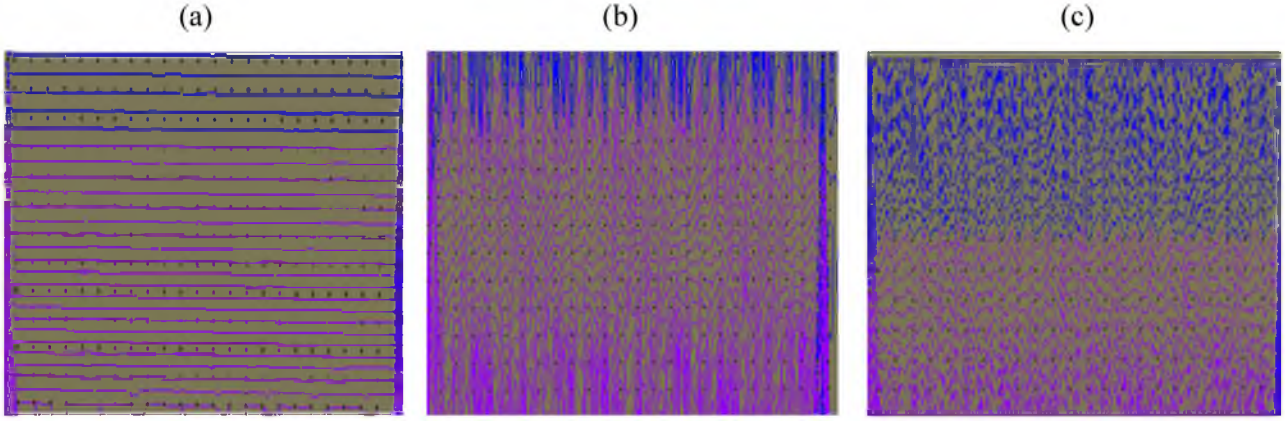

Figure 14: (a) TIN road traffic noise contour extract fit with Nops; (b) IDW road traffic noise contours that are in irregular shapes; (c) kriging road traffic noise contours that are in irregular shapes in 3D space.

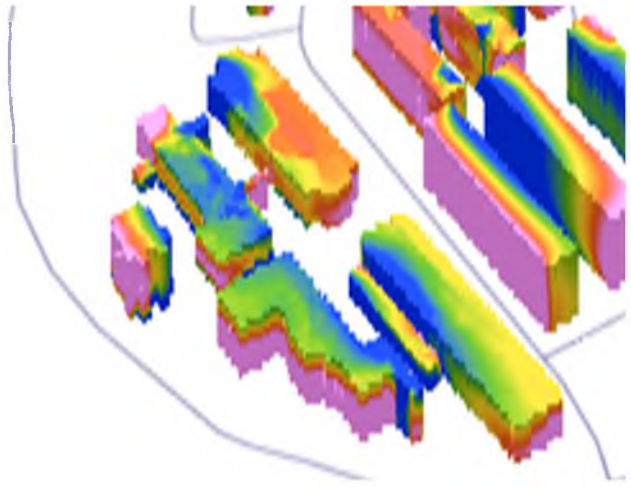

Figure 15: Irregular-shape voxel edges of 3D road traffic noise visualisation.

However, the 3D noise contours have irregular and unexpected shapes between the ground level and 1 m level of facades. This means that the Henk de Klujijver model does not show a more accurate value when the observation points are closer to ground level. However, it is not an issue; the 2D noise mapping assumes that the noise levels propagate above 1.5 m from ground level. The 3D noise contour visualisation and the 3D kriging voxel visualisation were used to validate the 3D noise visualisation. In 3D noise visualisation, 3D contours show that ME is −0.337 and RMSE is 0.658. 3D Kriging voxel shows that ME is −0.293 and RMSE is 0.425. Twenty-one sample noise points were taken on building facades for 3D validation. Changing noise levels is limited along the building facades in a vertical direction. The facades of only a few buildings are less than 55 dB(A). The shape of the building has a valid influence on road traffic noise levels [60]. However, in the results of this study, it can be concluded that the shape of the UTM buildings is not a valid influence for changes in noise levels in 3D space than in 2D. If the study area is flat, it is not a complex process to design Nop. Moreover, in that case, the terrain height does not affect the receiver's height from the reference road level. Otherwise, the study area is undulated, and the terrain has a high impact on the receiver heights from the reference road level.

4 Conclusions

Road traffic noise levels vary with different types of factors. Physical and environmental conditions are the main factors that influence traffic noise levels. Many of those conditions, reflectance noise from building facades, noise mitigation from noise barriers, and weather conditions do not remain uniform. Therefore, the existing noise model requires modifications relevant to environmental conditions [4,61]. Furthermore, calculating the number of vehicles in a dynamic traffic flow is a difficult task. In this study, a manual vehicle calculation method was used. However, the study has developed a machine learning method to detect traffic flow using camera images. Thus, this method can be integrated into this current study to calculate the number of vehicles [23]. Road traffic noise propagates in all directions. Therefore, identifying the noise propagation path between the vehicle and the Nop is a difficult task, in a complex building environment. The diffraction occurs on the noise propagation path due to facades and horizontal and vertical edges of buildings. This means that buildings act as noise barriers between the noise source and the receiver [55]. However, there is no method for finding noise mitigation from building barriers. However, studies by Dudiev and Tupov [62] have shown an equation to find noise reduction from wall noise barriers. The width of the wall is not considered a factor in reducing noise. If there are straight-up slopes and straight-down slopes, the terrain may be noise barriers for propagation. Therefore, designing Nop beyond these slopes is not possible for noise calculations. There is no maximum distance to which traffic noise can travel. The maximum distance from Nop to the centreline of the road should be considered when designing Nop, and the maximum distance can be taken after field verification. However, according to the RMSE and ME of 2D noise interpolation, the kriging has the lowest RMSE and ME; in this case, kriging is vital to interpolate noise levels in 2D space (x and y). The TIN is vital for 3D noise visualisation. The inaccurate distribution of locations (Nops) impacts the final noise visualisation. Therefore, the number of sample noise points, the distribution, and the density of sample noise points should be considered. Still, it is a challenge to validate noise contours in 2D and 3D spaces. However, it is possible to validate noise contours after converting them onto raster surfaces. According to the 3D noise validation, the 3D kriging voxel was more accurate than the visualisation of 3D noise contours. But visualising traffic 3D kriging voxel is a more complex process than 3D contour visualisation. However, a 3D kriging voxel is more effective and accurate for 3D traffic noise visualisation. However, cartographical simplification is essential for voxel edges to eliminate irregular square shapes (Figure 15).

Uncertainty errors occur when the output cell sizes may not match the accuracy of the noise levels. Furthermore, if the resolution of 2D and 3D buildings (building dimension) is not related to the size of noise visualisation, it is a reason for inaccurate traffic noise visualisation [63]. Noise pollution is a phenomenon, and colour is a visual variable that

represents a phenomenon. In traffic noise visualisation, the intensity of warm colour decreased, and cool colour was used to represent higher noise levels. In that case, purple is used for higher noise levels, and light blue is used to represent lower noise levels. It may be the reason why the red and green colour cannot be easily identified by 0.5% of female and 8% of male persons [64]. Therefore, enhancing the green to light blue and the red to purple is a solution to avoid that matter.

Acknowledgments: This work was supported by the Ministry of Higher Education through Fundamental Research Grant Scheme (FRGS/1/2022/WAB07/UTM/02/3). This study was carried out in accordance with the specifications and recommendations of the 3D GIS Research Lab at Universiti Teknologi Malaysia.

Author contributions: Each author has agreed to be accountable for the full manuscript's content and has given their approval for submission.

Conflict of interest: The authors claim there is no conflict of interest.

References

[1] Peng J, Parnell J, Kessissoglou N. Spatially differentiated profiles for road traffic noise pollution across a state road network. Appl Acoust. 2021;172:107641.
[2] Ruiz-Padillo A, Ruiz DP, Torija AJ, Ramos-Ridao A. Selection of suitable alternatives to reduce the environmental impact of road traffic noise using a fuzzy multi-criteria decision model. Environ Impact Assess Rev. 2016;61:8–18.
[3] Ruiz-Padillo A, Torija AJ, Ramos-Ridao AF, Ruiz DP. Application of the fuzzy analytic hierarchy process in multi-criteria decision in noise action plans: Prioritizing road stretches. Environ Model Softw. 2016;8:45–55.
[4] Munir S, Khan S, Nazneen S, Ahmad SS. Temporal and seasonal variations of noise pollution in urban zones: a case study in Pakistan. Environ Sci Pollut Res. 2021;28(23):29581–9.
[5] Partheeban P, Karthik K, Elamparithi PN, Somasundaram K, Anuradha B. Urban Road traffic noise on human exposure assessment using geospatial technology. Environ Eng Res. 2021;27(5):210249.
[6] Rey G, Gómez V. Uncertainty evaluation of road traffic noise models in two Ibero- American cities. Appl Acoust. 2021;180:108134.
[7] Debnath A, Singh PK. Environmental traffic noise modelling of Dhanbad township area – A mathematical based approach. Appl Acoust. 2018;129:161–72.
[8] Harman BI, Koseoglu H, Yigit CO. Performance evaluation of IDW, kriging and multiquadric interpolation methods in producing noise mapping: A case study at the city of Isparta Turkey. Appl Acoust. 2016;112:147–57.
[9] Kurakula VK, Kuffer M. 3D noise modeling for urban environmental planning and management. Real Corp 008. 2008;2:517–23.
[10] Rajakumara HN, Gowda RMM. Road traffic noise prediction models: A Review. Int J Sustain Dev Plan. 2008;3(3):257–71.
[11] Weninger B. A colour scheme for the presentation of sound emission in maps: Re-quirements and principles for design. Euro Noise. 2015;439–44.
[12] Puyana-Romero V, Cueto JL, Gey R. A 3D GIS tool for the detection of noise hot-spots from major roads. Transp Res D: Transp Environ. 2020;84:102376.
[13] Licitra G, Bolognese M, Chiari C, Carpita S, Fredianelli L. Noise Source Predominance Map: a new representation for strategic noise maps. Noise Mapp. 2022;9(1):269–79.
[14] Ascari E, Cerchiai M, Fredianelli L, Licitra G. Statistical pass-by for unattended road traffic noise measurement in an urban environment. Sensors. 2022;22(22):8767.
[15] Del Pizzo LG, Teti L, Moro A, Bianco F, Fredianelli L. Influence of texture on tyre road noise spectra in rubberized pavements. Appl Acoust. 2020;159:1–12.
[16] Teti L, De León G, Del Pizzo LG, Moro A, Bianco F, Fredianelli L, et al. Modelling the acoustic performance of newly laid low-noise pavements. Constr Build Mater. 2020;247:118509.
[17] Moreno R, Bianco F, Carpita S, Monticelli A, Fredianelli L, Licitra G. Adjusted controlled pass-by (CPB) method for urban road traffic noise assessment. Sustainability. 2023;15(6):5340.
[18] Ramos-Romero C, Asensio C, Moreno R, de Arcas G. Urban road surface discrimination by tire-road noise analysis and data clustering. Sensors. 2022;22:9686.
[19] Filho JMA, Lenzi A, Zannin PHT. Effects of traffic composition on road noise: A case study. Transp Res D: Transp Environ. 2004;9(1):75–80.
[20] Ranjbar HR, Gharagozlou AR, Reza A, Nejad V. 3D analysis and investigation of traffic noise impact from Hemmat highway located in Tehran on buildings and surrounding areas. J Geogr Inf Syst. 2012;4(4):311–34.
[21] Praticò FG. On the dependence of acoustic performance on pavement characteristics. Transp Res D: Transp Environ. 2014;29:79–87.
[22] Mishra RK, Mishra AR, Singh A. Traffic noise analysis using RLS-90 model in urban city. INTER-NOISE: Noise Control for a Better Environment; 2019 Jun 16–19; Madrid, Spain. Spanish Acoustical Society, 2019. p. 6490–502.
[23] Fredianelli L, Carpita S, Bernardini M, Del Pizzo LG, Brocchi F, Bianco F, et al. Traffic flow detection using camera images and machine learning methods in ITS for-Noise map and action plan optimization. Sensors. 2022;22(5):1929.
[24] Yang W, He J, He C, Cai M. Evaluation of urban traffic noise pollution based on noise maps. Transp Res D: Transp Environ. 2020;87:102516.
[25] Halfwerk W, Holleman LJM, Lessells CM, Slabbekoorn H. Negative impact of traffic noise on avian reproductive success. J Appl Ecol. 2011;48(1):210–9.
[26] Gulliver J, Morley D, Vienneau D, Fabbri F, Bell M, Goodman P, et al. Development of an open-source road traffic noise model for exposure assessment. Environ Model Softw. 2015;74:183–93.
[27] Nejad PG, Ahmad A, Zen IS. Assessment of the Interpolation techniques on traffic noise pollution mapping for the campus environment sustainability. Int J Built Environ Sustain. 2019;6(1–2):147–59.
[28] Che D, Jia Q. Three-dimensional geological modeling of coal seams using weighted Kriging method and multi-source data. IEEE Access. 2019;7:118037–45.
[29] Chesnaux R, Lambert M, Walter J, Fillastre U, Hay M, Rouleau A, et al. Building a geodatabase for mapping hydrogeological features

and 3D modeling of groundwater systems: Application to the Saguenay-Lac-St.-Jean region. Comput Geosci. 2011;37(11):1870–82.
[30] Delsman JR, Van Baaren ES, Siemon B, Dabekaussen W, Karaoulis MC, Pauw PS, et al. Large-scale, probabilistic salinity mapping using airborne electromagnetics for groundwater management in Zeeland, the Netherlands. Environ Res Lett. 2018;13(8):084011.
[31] Cai M, Yao Y, Wang H. Urban traffic noise maps under 3D complex building environments on a supercomputer. J Adv Transp. 2018;2018:7031418.
[32] Pamanikabud P, Tansatcha M. Geographical information system for traffic noise analysis and forecasting with the appearance of barriers. Environ Model Softw. 2003;18(10):959–73.
[33] Saglam A, Makineci HB, Baykan NA, Baykan ÖK. Boundary constrained voxel segmentation for 3D point clouds using local geometric differences. Expert Syst Appl. 2020;157:113439.
[34] Wu H, Zhu Q, Guo Y, Zheng W, Zhang L, Wang Q, et al. Multi-level voxel representations for digital twin models of tunnel geological environment. Int J Appl Earth Obs Geoinf. 2022;112:102887.
[35] Li J, Liu P, Wang X, Cui H, Ma Y. 3D geological implicit modeling method of regular voxel splitting based on layered interpolation data. Sci Rep. 2022;12(1):1–14.
[36] Grunwald S, Barak P, Rooney D. Web-based virtual models for the earth science community. ASAE International Meeting in Sacramento; 2001. p. 013029.
[37] Venkataraman S, Falls S. Voxel-based analysis and visualization of rainfall data. Pecora 16 Global Priorities in Land Remote Sensing; 2005 Oct 23–25; Sioux Falls (SD), USA. American Society for Photogrammetry and Remote Sensing, 2005.
[38] Wang G, Pang Z, Boisvert JB, Hao Y, Cao Y, Qu J. Quantitative assessment of mineral resources by combining geostatistics and fractal methods in the Tongshan porphyry Cu deposit (China). J Geochem Explor. 2013;134:85–98.
[39] Harona Z, Han LM, Darus N, Lee YL, Jahya Z, Hamid MFA, et al. A preliminary study of environmental noise in public university. J Teknologi. 2015;77(16):145–51.
[40] Bocher E, Guillaume G, Picaut J, Petit G, Fortin N. Noise modelling: An open-source GIS based tool to produce environmental noise maps. ISPRS Int J Geo-Information. 2019;8(3):130.
[41] Lesieur A, Mallet V, Aumond P, Can A. Data assimilation for urban noise mapping with a meta-model. Appl Acoust. 2021;178:1–30.
[42] Zefreh MM, Torok A. Theoretical comparison of the effects of different traffic conditions on urban road environmental external costs. Sustainability. 2021;13(6):3541.
[43] Eggenschwiler K, Heutschi K, Taghipour A, Pieren R, Gisladottir A, Schäffer B. Urban design of inner courtyards and road traffic noise: Influence of façade characteristics and building orientation on perceived noise annoyance. Build Environ. 2022;224:109526.
[44] Orchard SO, Anifantis AS, Camposeo S, Vivaldi GA, Santoro F, Pascuzzi S. Comparison of UAV photogrammetry and 3D modeling techniques with other currently used methods for estimation of the tree row volume of a super-high-density olive orchard. Agriculture. 2019;9:233.
[45] Hood RA. Calculation of road traffic noise. Appl Acoust. 1987;21:139–46.
[46] ISO. ISO 9613-2:1996. Acoustics - Attenuation sound Propag outdoors - Part 2: General method of calculation. 1996;1.
[47] Attenborough K, Bashir I, Taherzadeh S. Exploiting ground effects for surface transport noise abatement. Noise Mapp. 2016;3(1):1–25.
[48] Tang JH, Lin BC, Hwang JS, Chen LJ, Wu BS, Jian HL, et al. Dynamic modeling for noise mapping in urban areas. Environ Impact Assess Rev. 2022;97:106864.
[49] Chenaux A, Murphy M, Pavia S, Fai S, Molnar T, Cahill J, et al. A review of 3D GIS for use in creating virtual historic Dublin. Int Arch Photogramm, Remote Sens Spat Inf Sci. 2019;42(2/W9):249–54.
[50] Alomía G, Loaiza D, Zúñiga C, Luo X, Asorey-Cacheda R. Procedural modeling applied to the 3D city model of bogota: a case study. Virtual Real Intell Hardw. 2021;3(5):423–33.
[51] Peng J, Bullen R, Kean S. The effects of vegetation on road traffic noise. INTER-NOISE: Improving the World Through Noise Control; 2014 Nov 16–19; Melbourne, Australia. Australian Acoustical Society, 2014.
[52] Angjeliu G, Coronelli D, Cardani G. Development of the simulation model for Digital Twin applications in historical masonry buildings: The integration between numerical and experimental reality. Comput Struct. 2020;238:106282.
[53] Pinos J, Vozenilek V, Pavlis O. Automatic geodata processing methods for real-world city visualizations in cities: Skylines. ISPRS Int J Geo-Information. 2020;9(1):17.
[54] Barrile V, Candela G, Fotia A. Point cloud segmentation using image processing techniques for structural analysis. Int Arch Photogramm, Remote Sens Spat Inf Sci. 2019;42(2/W11):187–93.
[55] Zhao W, Liu E, Joo H, Wang B, Gao S, Eng C, et al. 3D traffic noise mapping using unstructured surface mesh representation of buildings and roads. Appl Acoust. 2017;127:297–304.
[56] Li J, Heap AD. Spatial interpolation methods applied in the environmental sciences: A review. Environ Model Softw. 2014;53:173–89.
[57] Li H, Xie H. Noise exposure of the residential areas close to urban expressways in a high-rise mountainous city. Environ Plan B: Urban Analytics City Sci. 2021;48(6):1414–29.
[58] Salsabili M, Saeidi A, Rouleau A, Nastev M. 3D probabilistic modelling and uncertainty analysis of glacial and post-glacial deposits of the city of Saguenay. Can Geosci. 2021;11(5):1–21.
[59] Sygna K, Aasvang GM, Aamodt G, Oftedal B, Krog NH. Road traffic noise, sleep and mental health. Environ Res. 2014;131:17–24.
[60] Lu L, Becker T, Löwner MO. 3D complete traffic noise analysis based on CityGML. In: Abdul-Rahman A, editors. Advances in 3D Geoinformation. Lecture Notes in Geoinformation and Cartography. Springer, Cham. 2017. p. 265–283.
[61] Rochat JL, Reiter D. Highway traffic noise. Acoust Today. 2016;12(4):38–47.
[62] Dudiev T, Tupov V. Method of acoustic calculation of traffic noise barriers. MATEC Web Conf. 2020;320:00034.
[63] Gozalo GR, Escobara VG. Uncertainty evaluation of road traffic noise models in two Ibero-American cities. Appl Acoust. 2012;180:108134.
[64] Atchison DA, Pedersen CA, Dain SJ, Wood JM. Traffic signal color recognition is a problem for both protan and deutan color-vision deficients. Hum Factors. 2003;45(3):495–503.